Transactions, SMiRT-24
BEXCO, Busan, Korea - August 20-25, 2017
Division IX (include assigned division number from I to X)

ANCHOARGE STRENGTH OF 550MPA 43MM HOOKED BARS IN JOINTS

Sungchul Chun[1], Mun-Gil Kim[2], Hye-Jung Sim[2], and Byung-Soo Lee[3]

[1] Associate Professor, Division of Architecture and Urban Design, Incheon National University, Korea
[2] Ph.D. Candidate, Division of Architecture and Urban Design, Incheon National University, Korea
[3] Senior Researcher, Central Research Institute, Korea Hydro & Nuclear Power Co. Ltd, Korea

ABSTRACT

In the construction of nuclear power plants, only 420 MPa reinforcing bars are allowed and, therefore, so many large-diameter bars are placed, which results in steel congestion. Consequently, re-bar works are difficult and the quality of RC structures may be deteriorated. To solve the steel congestion, 550 MPa bars are necessary. Among many items for verifying structural performance of reinforced concrete with 550 MPa bars, the 43 mm hooked bars are examined in this study. All specimens failed by side-face blowout and the side cover explosively spalled at maximum loads. The bar force was initially transferred to the concrete primarily by bond along a straight portion. At the one third of maximum load, the bond reached a peak capacity and began to decline, while the hook bearing component rose rapidly. At failure, most load was resisted by the hook bearing. For confined specimens with hoops, the average value of test-to-prediction ratios by KCI code is 1.45. The modification factor of confining reinforcement which was not allowed for larger than 35 mm bars can be applied to 43 mm hooked bars. For specimens with 70 MPa concrete, the average value of test-to-prediction ratios by KCI code is 1.0 which is less than the values of the other specimens. The effects of concrete compressive strength should be reduced.

INTROUDCITON

The ACI 318-14 (2014), ACI 349-13 (2013), and ASME Code (2015) allow for the usage of 43 and 57 mm hooked bars but the structural behavior and anchorage strengths of the 43 and 57 mm hooked bars have not been experimentally evaluated. From 1970s, several studies (Minor and Jirsa 1975, Marques and Jirsa 1977, Pinc et al. 1977, Johnson and Jirsa 1981, Soroushian et al. 1988, Hamad et al. 1993, Joh and Shibata 1996) were conducted on the hooked bars and the largest bar diameter is 36 mm. The confining effects of the cover and transverse reinforcement are excluded in the ACI 318 provisions on the development lengths of the 43 and 57 mm hooked bars because of the absence of experimental evidence. The demand for the high-strength reinforcement of 550 MPa yield strength has increased, resulting in a reduction of the material costs and steel congestion, in particular in the construction of nuclear power plants and tall buildings.

Simulated beam-column joint tests were conducted using 550 MPa hooked bars of 43 mm to investigate the effects of the design variables on the anchorage strengths of the hooked bars.

EXPERIMENTAL PROGRAM

Specimen Variables

A typical specimen simulating an exterior beam-column joint is shown in Fig. 1. Two hooked bars were embedded as beam longitudinal bars into the column, which is horizontally positioned for the safe test. The embedment length and side-cover were designed so that a side-face blowout failure occurred before the headed bars yielded. From an overview of the design-code provisions (ACI 318-14

2014, ACI 349-13 2013, and ASME Code 2015) and previous research (Minor and Jirsa 1975, Marques and Jirsa 1977, Pinc et al. 1977, Johnson and Jirsa 1981, Soroushian et al. 1988, Hamad et al. 1993, Joh and Shibata 1996, Sperry et al. 2015) on hooked bars, the main variables affecting the anchorage strength of headed bars terminated within an exterior beam-column joint are determined as follows: bar diameter d_b, embedment length l_{dh}, side cover thickness c_{so}, compressive strength of concrete f_c', and confining transverse reinforcement.

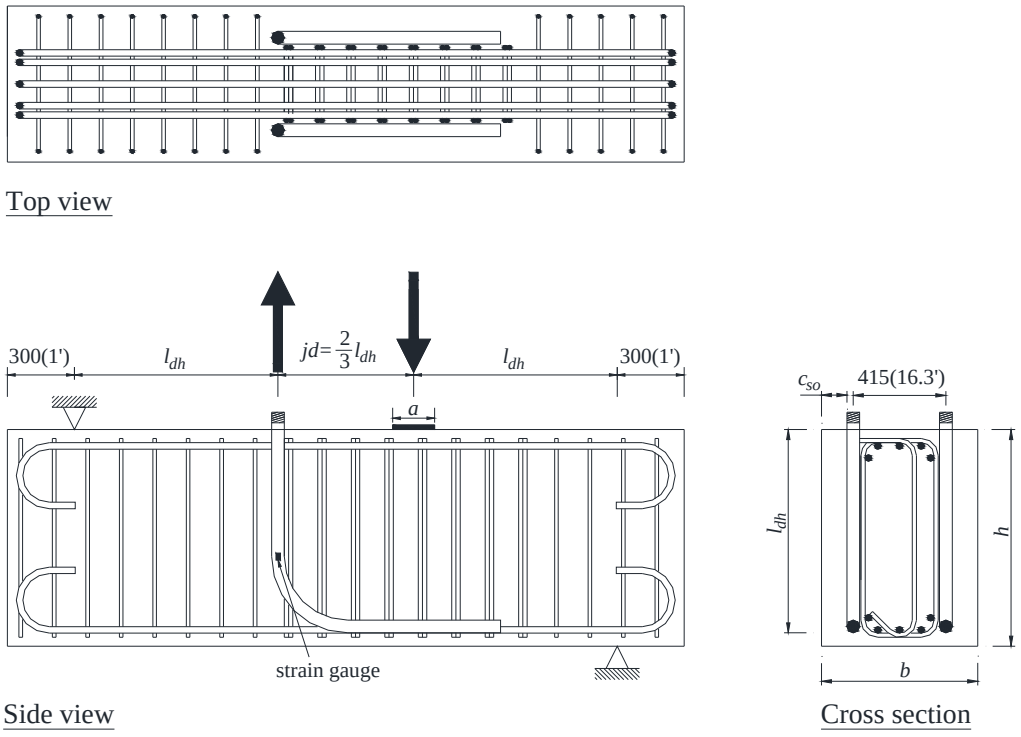

Figure 1. Specimen details.

Bar diameter of 43 mm, which is larger than the largest bar used in the previous researches (Minor and Jirsa 1975, Marques and Jirsa 1977, Pinc et al. 1977, Johnson and Jirsa 1981, Soroushian et al. 1988, Hamad et al. 1993, Joh and Shibata 1996, Sperry et al. 2015), was tested. The embedment length varied from $10d_b$ to $20d_b$; this range of embedment lengths was chosen to ensure that the anchorage would fail before the hooked bars could actually yield. Two types of clear side-cover value were tested, as follows: $1d_b$ which simulates a practical side-cover thickness for 43 mm-diameter headed bars, and $2d_b$ which may be a maximum value for the inside bar in a case where vertical and horizontal bars are simultaneously placed in walls. Two types of concrete compressive strength, with design values of 42 MPa and 70 MPa, were used. The compressive strengths of concrete, tested in accordance with ASTM C39/C39M-14 (2014) at the test date, are summarized in Table 1.

For the unconfined specimens of Figure 1, the ties along the tails of the hooked bars were placed within the two hooked bars and consequently no reinforcing bars were placed between an anticipated failure surface and the hooked bar. For the confined specimens, the hooked bars were enclosed within the ties parallel to the hooked bars. The amounts of the transverse reinforcement are shown in Table 1 in terms of the transverse reinforcement index K_{tr} calculated according to Eq. (25.4.2.3b) of ACI 318-14 (2014).

Table 1: Test matrix and results.

Specimen ID*	$\frac{l_{dh}}{d_b}$	$\frac{c_{so}}{d_b}$	f_c' MPa	h mm	a mm	Transverse reinforcement $[K_{tr}/d_b]$	$f_{dh,e}$, MPa (ksi)	
							Bar 1	Bar 2
D43-L10-C1-S42	10	1	44.4	480	130	-	297	410
D43-L10-C1-S42-C	10	1	47.9	480	130	2D19@120 [2.22]	491	543
D43-L10-C1-S70	10	1	69.0	480	130	-	315	440
D43-L10-C2-S42	10	2	48.4	480	130	-	361	445
D43-L13-C1-S42	13	1	48.4	609	146	-	388	500
D43-L13-C1-S42-C	13	1	48.4	609	146	2D19@130 [2.05]	494	552
D43-L13-C1-S70	13	1	73.1	609	130	-	428	445
D43-L13-C2-S42	13	2	48.4	609	146	-	466	480
D43-L16-C1-S42	16	1	48.4	738	170	-	525	476
D43-L16-C1-S42-C	16	1	48.4	738	170	2D19@130 [2.05]	560	528
D43-L16-C1-S70	16	1	69.0	738	146	-	545	513
D43-L16-C2-S42	16	2	48.4	738	170	-	577	538
D43-L20-C1-S42	20	1	48.4	926	190	-	582	541

* D①- L②-C③-S④-⑤: ① is the bar diameter in mm; ② is the embedded length normalized by the bar diameter; ③ is the side cover normalized by the bar diameter; ④ is the design compressive strength of concrete in MPa; "a" and "b" of ⑤ refer to the duplicate specimens; and "C" of ⑤ refers to the confined specimen by transverse reinforcement.

In all of the specimens, the confinement influence of the longitudinal column bars was excluded by placing the column bars between the two headed bars as shown in Figure 1. This reinforcement arrangement is somewhat conservative compared with the conventional bar arrangement. In case that a beam width is wider than a column width, the longitudinal bars and ties of the column cannot confine the headed bars used as beam longitudinal bars. A total of thirteen specimens were tested and the variables of each specimen are summarized in Table 1.

Specimen Design, Test Setup, and Instrumentation

Specimens were designed to represent exterior beam-column joints and were cast without the beam. Because the side-face blowout failure was anticipated, the other failures were prevented. By providing sufficient joint area and ties in the joint, the joint shear strengths of the specimens were enough to resist the joint shear demands until the headed bars yielded. The joint area was designed in accordance with ACI 352R-02 (2002) with γ = 15 for the Type 1 corner joint. To prevent the concrete breakout failure, the ratio of the internal moment arm of the beam jd to the embedment length l_{dh} was designed to be 2/3, as shown in Figure 1 in compliance with R25.4.4.2 of ACI 318 (2014).

The amount of the column longitudinal bars was determined so that the column bars remain elastic until the headed bars yielded. The cover beyond the hook was minimized as the sum of the minimum cover of 40 mm and the tie diameter to increase the ratio of the embedment length (l_{dh}) to the column depth (h). The specimen lengths were chosen so that the joint shear force is higher than the column shear force to simulate the headed bars anchored in an exterior beam-column joint as shown in Figure 1. In this study, the joint shear force is three times the column shear force.

The design yield strengths of the hooked bars are all 550 MPa and the measured yield and tensile strengths of the 43 mm hooked bars are 620 MPa and 782 MPa, respectively. The strengths of the hooked bars meet the tensile requirements of ASTM A706-14 (2014) and A615-15 (2015).

The test setup is designed to examine the anchorage of hooked bars used as the longitudinal beam reinforcement in an exterior beam-column joint as shown in Figure 2. The test setup is notably similar to that of the hooked bar tests conducted by Marques and Jirsa (1977) from which the ACI 318 provisions (2014) for hooked bars were developed. The test setup used in this study differs from that used by Marques and Jirsa (1977) in two ways: no axial load was applied to the column because the axial load can increase the anchorage capacity of the headed bars and, for safety, the specimens were tested with the column in a horizontal position. Tensile forces were applied monotonically to the hooked bars, which extended past the reaction frame, using hydraulic rams with a capacity of 3000 kN to simulate the tensile forces in the beam reinforcement at the face of a beam-column joint. The compression zone of the beam was duplicated with a steel plate bearing against the face of the column. The compression depth indicated, as *a* in Figure 1, was determined based on the elastic analysis and its values are shown in Table 1. The vertical supports at the left and right of the columns simulated the inflection points of the upper and lower columns, respectively.

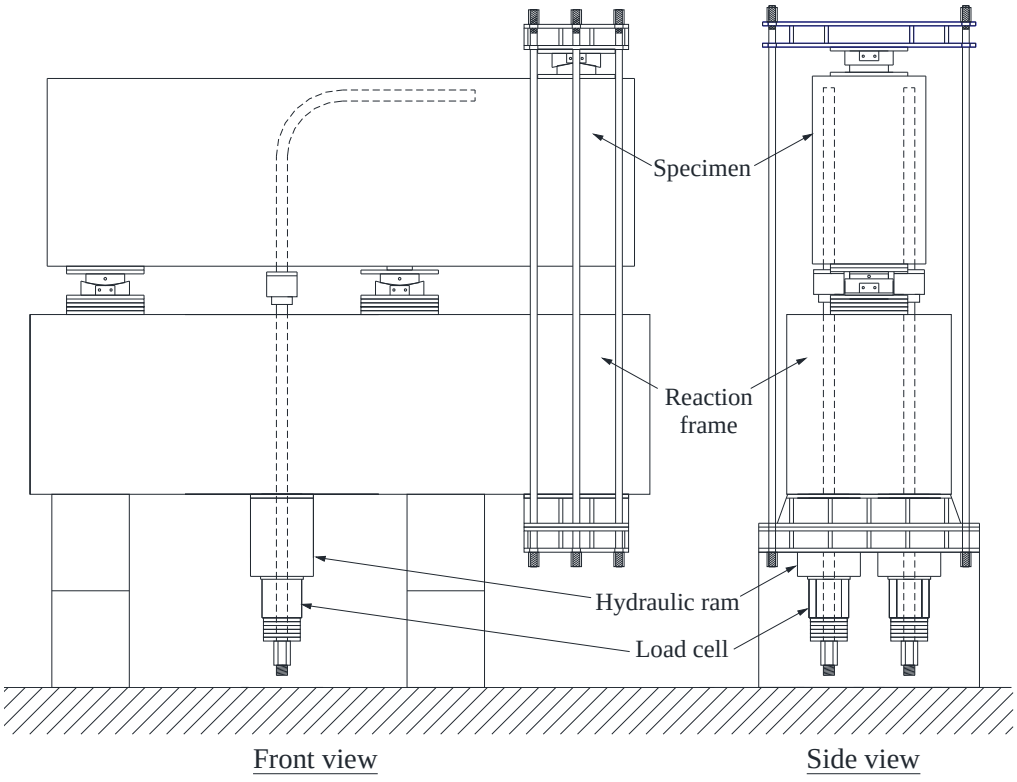

Figure 1. Test setup.

The applied loads were directly measured using load cells mounted on the hydraulic rams. To determine the hook bearing and bond contributions, electrical resistance strain gauges were attached at the starting points of the hooks as shown in Figure 1. Two gauges were used at each measurement point on both sides of the bar to diminish any flexure contribution to the strain.

TEST RESULTS

Overall Behavior and Failure Modes

Cracking most often began with a vertical crack on the front face of the column along the straight portion of the hooked bars. This cracking is considered to be caused by the bond failure. In addition, the cracking is also caused by a flexural moment in the column, since the flexural moment at the point where the hooked bars are embedded is the highest. The vertical crack propagated toward the hook as the load increased. A few inclined cracks between the hooked bar and the compression reactions also formed. At a maximum load, the cover concrete around the hooks suddenly spalled as shown in Figure 3 and the load dropped immediately. The main cause of the failure is the spalling of the side cover concrete around the hook and is very similar to the side-face blowout failure of anchors (Furche and Eligehausen 1991) and headed bars (Chun et al. 2017). All specimens showed the same crack pattern and failure mode.

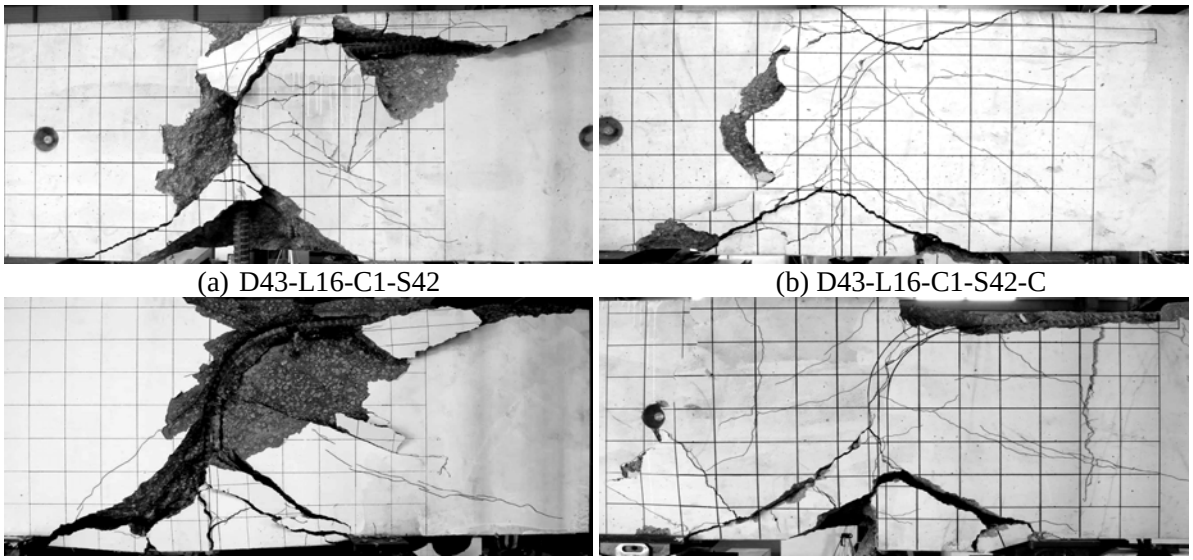

(a) D43-L16-C1-S42 (b) D43-L16-C1-S42-C

(c) D43-L16-C1-S70 (d) D43-L16-C2-S42

Figure 3 Typical specimen failures of D43-L16-series. (Bae et al. 2016)

Developed Bar Stresses

The anchorage strengths $f_{dh,e}$ (i.e. the developed stresses at the time of failure) were directly obtained by dividing the measured loads by the cross sectional area of the hooked bars and are summarized in Table 1. Equation (1) modified from the design equation of ACI 318 (2014) shows the relationship between the bar stress and given the embedment length and compressive strength of concrete where the modification factors ψ_e, ψ_c, ψ_r, and λ are set as one.

$$f_{dh,ACI} = \frac{l_{dh}}{0.24 d_b}\sqrt{f_c'} \tag{1}$$

where $f_{dh,ACI}$ is the predicted bar stress based on the development length equation of ACI 318-14 (2014).

The measured bar stresses are compared with the predicted values from Eq. (1) in Figure 4(a). The hooked bars with a $1d_b$ side cover show anchorage strengths that are a little higher than the predictions by only 7% on average. Particularly, the hooked bars anchored in 70 MPa concrete have

almost the same anchorage strength as the predictions by Eq. (1). Considering the capacity reduction factor of 0.8 used in developing Eq. (1) (ACI Committee 408, 1979), the average of the test-to-prediction ratio is not sufficient which means that the current design code is not conservative for the 43 mm hooked bars with a side cover of $1d_b$. However, in case that the side cover increases to $2d_b$ or the transverse reinforcement is provided, the hooked bars have sufficient anchorage capacities and Eq. (1) provides the safe results. The side cover and the transverse reinforcement obviously affect the anchorage strength of hooked bars and these factors should be involved in the design equation of the development length of hooked bars.

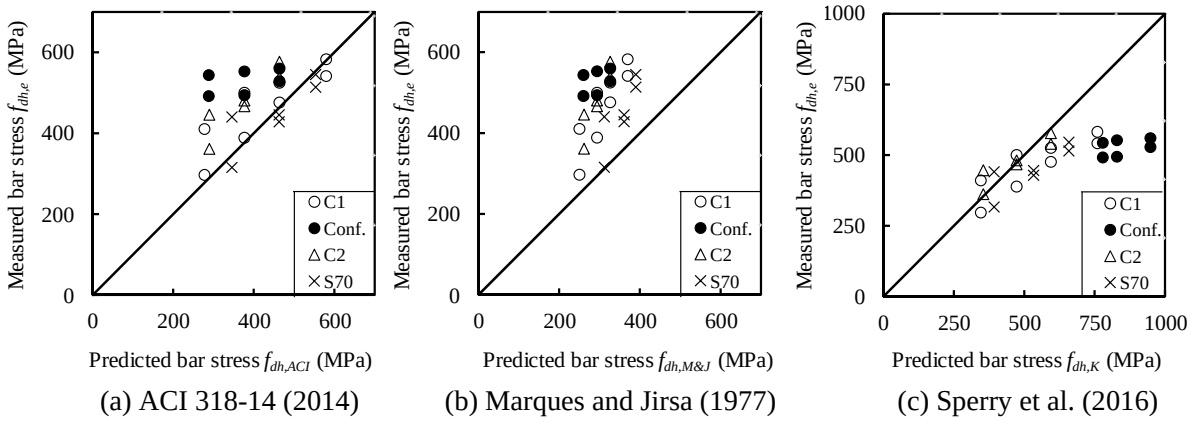

(a) ACI 318-14 (2014) (b) Marques and Jirsa (1977) (c) Sperry et al. (2016)

Figure 4 Comparisons of measured bar stresses with predictions.

Marques and Jirsa's Model (1977) significantly underestimates the anchorage strength of hooked bars and especially for the hooked bars with a $2d_b$ side cover and the hooked bars confined with the transverse reinforcement, the test-to-prediction ratios are greater than 2.0 as shown in Figure 4(b). Marques and Jirsa (1977) proposed the modification factor ψ for the bars with a sufficient cover and transverse reinforcement but the factor can be applied to only 36 mm or smaller bars because of the absence of any test evidence for those larger than 36 mm. The comparison in Figure 4(b) shows that the side cover and transverse reinforcement are also favorable in the 43 mm hooked bars.

The calculated strengths by Sperry et al. (2016) are shown in Figure 4(c). The equations soundly predicted the hooked bar strength with the side cover of $2d_b$; however, the strengths of the hooked bars with the $1d_b$ side cover were overestimated because most tests conducted at Kansas University (Sperry et al. 2016) used sufficient side covers of more than $2.0d_b$ except for a few specimens and the equations do not consider the effects of the side cover. The equations include the effects of the bar diameter. Therefore, as the bar diameter increases from 43 mm, the ratio of test-to-prediction does not decrease but rather the test-to-prediction ratio increases slightly. The confined specimens with the transverse reinforcement are significantly overestimated. The failure modes of the Kansas University tests (Sperry et al. 2016) include various types of the front pullout, front blowout, side splitting, side blowout, and tail kickout and the model was derived from all kinds of failures. The failure strengths of the front pullout, front blowout, side splitting, and tail kickout are more sensitive to the confining transverse reinforcement than those of the side-face blowout because these failure modes are related to the joint shear failure. Consequently, the model overestimates the side-face blowout strength of the hooked bar with the confining transverse reinforcement.

These comparisons show that the anchorage capacity of hooked bars greatly depends on the failure mode, side cover, and transverse reinforcement.

Bond and Hook Bearing Contributions

The bar stress consists of the bond and hook bearing contributions. The bar stresses developed by the hook bearing $f_{brg,e}$ were estimated from the measured strains at the beginning of the hook as shown in Figure 1. The bar stresses developed by the bond $f_{b,e}$ could be obtained by deducting the stresses developed by the head bearing from the bar stresses.

The bond and hook bearing components are plotted in Figure 5 for D43-L20-C1-S42. The early rise in the bond component shows that the bar force was initially transferred to the concrete primarily by the bond. The bond reached a peak capacity at the bar stress of about 200 MPa and began to decline, while the hook bearing component rose rapidly. At this point, diagonal cracks were observed between the hook and the compression reaction. At failure, all of the bond vanished and the entire bar force was resisted by the hook bearing. This behavior significantly differs from the behavior of headed bars (Thompson et al. 2005, 2006, and Chun 2015) where the bond remained until failure even though the ratios of the bond contribution to the bar stress varied depending on the geometry of the anchorage zone. Although the bond contribution almost disappeared at failure, this does not mean that the straight portion of a hooked bar does not affect the anchorage but that the embedment length is one of the key parameters influencing the anchorage strength of hooked bars.

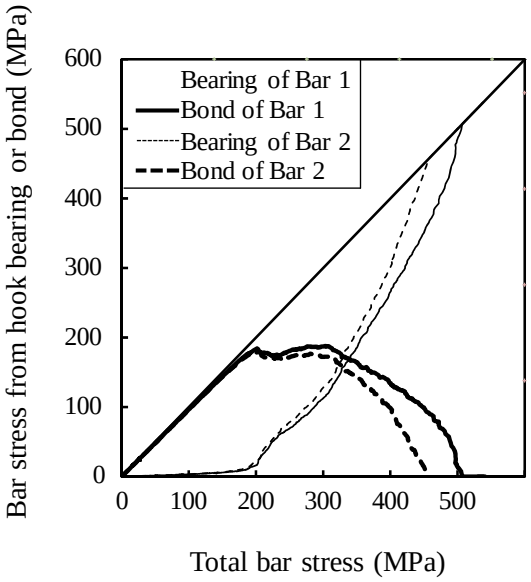

Figure 5 Bond and hook bearing components of anchorage strength of D43-L20-C1-S42.

CONCLUSIONS

Even though ACI 318 (2014) allows for the usage of 43 and 57 mm hooked bars, the structural behavior and anchorage strengths of the 43 and 57 mm hooked bars have not been experimentally evaluated. Simulated beam-column joint tests were conducted using 43 mm hooked bars of 550 MPa. The test variables include the embedment length, compressive strength of concrete up to 73.1 MPa, side cover of $1d_b$ and $2d_b$, and transverse reinforcement. Intentional side-face blowout failure occurred by preventing the other failure modes. The following conclusions can be drawn based on the test results:

1. As the embedment length and side cover increase, the anchorage capacity of hooked bars increases. By placing ties, the anchorage strengths of hooked bars increase but the increment highly scatters.

2. The anchorage strength consists of bond and head bearing contributions but, at failure, all of the bond vanished and the entire bar force was resisted by the hook bearing. Although the bond contribution almost disappeared at failure, the embedment length is one of the key parameters influencing the anchorage strength of hooked bars.

ACKNOWLEDGMENTS

This work was supported by Korea Hydro & Nuclear Power Co. Ltd (No. L16S140000).

REFERENCES

ACI Committee 318, *Building Code Requirements for Structural Concrete (ACI 318-14) and Commentary*, American Concrete Institute, Farmington Hills, Mich., 2014, 519.

ACI Committee 349, *Code Requirement for Nuclear Safety-Related Concrete Structures (ACI 349-13) and Commentary*, American Concrete Institute, Farmington Hills, Mich., 2013.

ACI-ASCE Joint Committee 352, *Recommendations for Design of Beam-Column Connections in Monolithic Reinforced Concrete Structures (ACI 352R-02)*, American Concrete Institute, Farmington Hills, Mich., 2002, 37.

ACI Committee 408, "Suggested Development, Splice, and Standard Hook Provisions for Deformed Bars in Tension," *Concrete International*, V. 1, No. 7, July 1979, 44-46.

ACI-ASME Joint Technical Committee, *Code for Concrete Containments*, The American Society of Mechanical Engineers, New York, NY, 2015, 188.

ASTM A605-15, *Standard Specification for Deformed and Plain Carbon-Steel Bars for Concrete Reinforcement*, West Conshohocken, PA., 2015, 8.

ASTM A706-14, *Standard Specification for Deformed and Plain Low-Alloy Steel Bars for Concrete Reinforcement*, West Conshohocken, PA., 2014, 7.

ASTM C39/C39M-14, *Standard Test Method for Compressive Strength of Cylindrical Concrete Specimens*, 2016 2016, 7.

Chun, S.-C., "Lap Splice Tests Using High-Strength Headed Bars of 550 MPa (80 ksi) Yield Strngth," *ACI Structural Journal*, V. 112, No. 6, Nov.-Dec. 2015, 679-688.

Chun, S.-C.; Choi, C.-S.; and Jung, H.-S., "Side-Face Blowout Failure of large-Diameter High-Strength Headed Bars in Beam-Column Joints," *ACI Structural Journal*, V. 114, No. 1, 2017. 161-172.

Furche, J. and Eligehausen, R., "Lateral Blow-Out Failure of Headed Studs Near a Free Edge," *Anchors in Concrete-Design and Behavior*, SP-130. 1991, American Concrete Institute, Farmington Hills, MI. 235-252.

Hamad, B. S.; Jirsa, J. O.; and Paulo, N. I. D. A. d., "Anchorage Strength of Epoxy-Coated Hooked Bars," *ACI Structural Journal*, V. 90, No. 2, Mar.-Apr. 1993, 210-217

Joh, O. and Shibata, T., "Anchorage Behavior of 90-Degree Hooked Beam Bars in Reinforced Concrete Beam-Column Joints," *Eleventh World Conference on Earthquake Engineering*, No. 1196 V. No. 1996, 8.

Johnson, L. A. and Jirsa, J. O., *The Influence of Short Embedment and Close Spacing on the Strength of Hooked Bar Anchorages*, Phil M. Ferguson Structural Engineering Laboratory, Department of Civil Engineering, The University of Texas at Austin, Austin, Texas, April 1981, 93.

Marques, J. L. G. and Jirsa, J. O., "A study of Hooked Bar Anchorages in Beam-Column Joints," *ACI Journal, Proceedings*, V. 72, No. 5, 1975, 198-209.

Minor, J. and Jirsa, J. O., "Behavior of Bent Bar Anchorage," *ACI Journal, Proceedings*, V. 72, No. 4, Mar.-Apr. 1975, 141-149.

Pinc, R. L.; Watkins, M. D.; and Jirsa, J. O., *Strength of Hooked Bar Anchorages in Beam-Column Joints*, Department of Civil Engineering / Structures Research laboratory, The University of Texas, Austin, Texas, 1977, 67.

Soroushian, P.; Obaseki, K.; nagi, M.; and Rojas, M. C., "Pullout Behavior of Hooked Bars in Exterior Beam-Column Connections," *ACI Structural Journal*, V. 85, No. 3, May-Jun 1988, 269-276.

Sperry, J.; Al-Yasso, S.; Searle, N.; DeRubeis, M.; Darwin, D.; O'Reilly, M.; Matamoros, A.; Feldman, L.; Lepage, A.; Lequesne, R.; and Ajaam, A., *Anchorage of High-Strength Reinforcing Bars with Standard Hooks*, University of Kansas, SM Report No. 111, Lawrence, June 2015, 243.

Thompson, M. K.; Ziehl, M. J.; Jirsa, J. O.; and Breen, J. E., "CCT Nodes Anchored by Headed Bars-Part 1: Behavior of Nodes," *ACI Structural Journal*, V. 102, No. 6, Nov.-Dec 2005, 808-815.

Thompson, M. K.; Ledesma, A.; Jirsa, J. O.; and Breen, J. E., "Lap Splices Anchored by Headed Bars," *ACI Structural Journal*, V. 103, No. 2, Mar.-Apr 2006, 271-279.